HOW SHAPE AFFECTS PLASMONIC PROPERTIES
OF METALLIC NANOSPHERES

T. SANDU[*], G. BOLDEIU
*National Institute for Research and Development in Microtechnologies, 126A,
Erou Iancu Nicolae street, 077190, Bucharest, ROMANIA*

Using a boundary integral equation method we analyze the extinction spectrum and the near-field enhancement induced by surface plasmon resonances with respect to the shape modifications of metallic nanospheres. We found that the shape effects are greater on near-field enhancement than on extinction. The far-field properties are affected by global geometric changes like the volume modifications. The near-field, however, is rather affected by targeted local shape variations like the curvature variation of nanosphere surface.

1. Introduction

Since its first practical application, the boundary integral equation (BIE) method has gained a lot of attention because it allows convenient calculations of the localized surface plasmon resonances (LSPRs) in metallic nanoparticles (NPs) [1]. The near-field properties as well as the far-field response depend on the eigenvalues and the eigenfunctions of the BIE operator [2, 3]. As a result the BIE method provides a quite clear picture of the LSPR physics and offers an analytical tool for the design of plasmonic nanostructures for various applications like sensing [4], imaging [5] or medical diagnosis [6].

In sensing applications there are two properties that are mainly used: (a) the shift of LSPRs by the change of the surrounding refractive index; and (b) the near-field enhancement of the impinging electromagnetic field around the metallic nanoparticles. Some design aspects of the shape changes have been treated in recent papers that calculate perturbatively [7,8] the variations of the LSPRs spectral locations with respect to shape changes. However, these papers [7,8] treated only the spectral shift of LSPRs but geometrical changes induce also changes in the coupling strength of the LSPRs to the electromagnetic field [9]. Thus shape variations change not only the positions of the LSPRs but also their strength and new LSPRs may emerge in the spectrum [9].

The BIE method also permits direct calculation of the near-field enhancement created by the LSPRs [3]. The near-field enhancement is potentially used in chemical detection with some spectroscopy techniques like surface enhanced Raman spectroscopy (SERS) and surface enhanced infrared spectroscopy (SEIRS) [10]. In other words, the LSPR effect enhances the applied electric field around the surface of metallic NPs, hence it enhances the Raman and the infrared molecular signature [11].

Advances made in chemical or top-down methods cannot avoid variations in shape or size [12]. Metallic nanospheres are ones of the most used plasmon NPs which are fabricated either by wet chemistry [10] or by plasma based techniques [13]. On the other hand, even though the nanospheres have good crystallinity their shape might deviate from a perfect sphere for instance due to the crystalline facets. Shape variations change not only the eigenvalues but also the eigenfunctions and their coupling weights to electromagnetic fields. In the present work we will analyze the changes of both the far-field spectrum and the near-field enhancement with respect to

---

* Corresponding author: titus.sandu@imt.ro

smooth shape variations from spherical shape. While the near-field and far-field spectrum are closely related [3], it will be shown that the near-field enhancement is more affected than the far-field spectrum by shape changes through local variations of the eigenfunctions responsible for plasmonic response of metallic nanospheres.

2. Method

In the BIE method it is used the quasi-static approximation, thus for a metallic NP of complex permittivity ϵ_i, bounded by a surface Σ, and embedded into a medium of permittivity ϵ_o, the surface charge density

$$u_{E_0} = \sum_k \frac{n_k E_0}{\frac{1}{2\lambda} - \chi_k} u_k \tag{1}$$

determines the LSPRs of NPs [2,3,14]. In eq. (1) $\lambda = (\epsilon_1 - \epsilon_0)/\epsilon_1 + \epsilon_0$, while χ_k is the kth eigenvalue of $\hat{M}$ and $\hat{M}^\dagger$, $n_k = \langle v_k | \boldsymbol{n} \cdot \boldsymbol{N} \rangle$ is the inner product defined on Σ, and u_k, and v_k are the eigenfunctions of $\hat{M}$ and its adjoint $\hat{M}^\dagger$, respectively. Also $\boldsymbol{n}$ is the normal to Σ and $\boldsymbol{E}_0 = E_0 \boldsymbol{N}$ is the applied field with E_0, the modulus of $\boldsymbol{E}_0$, the applied electric field. The operator $\hat{M}$ acting on a certain space of functions defined on Σ as

$$\hat{M}[u] = \frac{1}{4\pi} \int_{x,y \in \Sigma} \frac{u(y)\boldsymbol{n}(x)(x-y)}{|x-y|^3} d\Sigma_y \tag{2}$$

is not symmetric, but it can be symmetrized with the symmetric and positive operator [3]

$$\hat{S}[u] = \frac{1}{4\pi} \int_{y \in \Sigma} \frac{u(y)}{|x-y|} d\Sigma \tag{3}$$

via the Plemelj's symmetrization principle $\hat{M}^\dagger \hat{S} = \hat{S}\hat{M}$, which ensures the relationship between the eigenfunctions v_k and u_k by $v_i = \hat{S}[u_i]$. The surface charge density (1) allows us the calculation of both the far-field behavior provided by the extinction spectrum and the near-field enhancement [2, 3]. For instance, the specific polarizability α (the polarizability of the nanoparticle devided by its volume V) can be calculated from (1) as an eigenmode sum by

$$\alpha = \sum_k \frac{w_k}{\frac{1}{2\lambda} - \chi_k}. \tag{4}$$

In eq. (4) $w_k = \langle x \cdot \boldsymbol{N} | u_k \rangle \langle v_k | \boldsymbol{n} \cdot \boldsymbol{N} \rangle / V$ is the coupling weight to the incident light [2,3]. Equation (4) allows an analytic expression for α when the dielectric permittivity of the metallic NP is described by the Drude model of the form $\epsilon(\omega) = \varepsilon_m - \omega_p^2/(\omega(\omega + i\gamma))$, . Here ε_m is an essentially constant that includes the metallic interband contribution, ω_p is the plasma frequency, γ is the dumping constant. The embedding medium is considered as a real and constant dielectric permittivity ε_d. The specific polarizability α of the NP takes the following form [2]

$$\alpha(\omega) = \sum_k \frac{p_k(\varepsilon_m - \varepsilon_d)}{\varepsilon_k} - \frac{p_k}{1/2 - \chi_k} \frac{\varepsilon_d}{\varepsilon_k} \frac{\tilde{\omega}_{pk}^2}{\omega(\omega + i\gamma) - \tilde{\omega}_{pk}^2} \tag{5}$$

where $\tilde{\omega}_{pk} = \omega_p \sqrt{(1/2 - \chi_k)/\varepsilon_k}$ is the frequency associated with the localized plasmon resonance frequency and $\varepsilon_k = (1/2 + \chi_k)\varepsilon_d + (1/2 - \chi_k)\varepsilon_m$. The quantity α characterizes the far-field response of the nanoparticle, such that its imaginary part is proportional to the cross-section extinction of the incident light [10]

$$C_{ext} = \frac{2\pi}{\lambda} \text{Im}(\alpha V). \tag{6}$$

Hence, the eigenmodes whose w_k does not vanish are considered bright modes, while those eigenmodes with vanishing w_k (or below to a few percent points [9]) are considered dark modes that usually cannot be detected in the far-field spectrum.

The near-field and in general the field configuration in any point in the outer space of the nanoparticle can be found by calculating the field generated by the induced charge u_{E_0}. However, the near-field next to the NP surface Σ is directly related to the eigenfunctions of $\hat{M}$ and $\hat{M}^\dagger$ [3]. If the surface Σ is locally parameterized as $x = X(\xi_1, \xi_2)$, $y = Y(\xi_1, \xi_2)$, $z = Y(\xi_1, \xi_2)$, where ξ_1, ξ_2 are independent parameters and X, Y, and Z, are smooth functions, one can define the tangent vectors, $t_{\xi_{1,2}} = \frac{\partial r}{\partial \xi_{1,2}}/h_{\xi_{1,2}}$, and the normal to Σ, $n = t_{\xi_1} \times t_{\xi_2}$, such that $(t_{\xi_1}, t_{\xi_2}, n)$ generate an orthonormal three-frame. The norms $h_{\xi_{1,2}} = \left|\frac{\partial r}{\partial \xi_{1,2}}\right|$ are the Lamé coefficients of the surface. It can be shown that in the three-frame $(t_{\xi_1}, t_{\xi_2}, n)$ the electric field enhancement along the normal is [3]

$$E_n(\xi_1, \xi_2) = \sum_k \frac{n_k(\chi_k + 1/2)}{\frac{1}{2\lambda} - \chi_k} u_k(\xi_1, \xi_2) \tag{7}$$

and the field enhancement into the tangent plane has the following expression

$$E_t(\xi_1, \xi_2) = -\sum_{\substack{k; \\ i=1,2}} \frac{n_k}{\frac{1}{2\lambda} - \chi_k} \frac{1}{h_{\xi_i}} \frac{\partial v_k(\xi_1, \xi_2)}{\partial \xi_i} t_{\xi_i}. \tag{8}$$

Equations (7) and (8) provide a modal decomposition of the near-field enhancement and an intuitive and a direct relationship between the far-field [Eqs. (4)-(6)] and the near-field enhancement [Eqs. (7) and (8)]. Both the far-field and the near-field enhancement can be explicitly described by calculating χ_k, u_k, and v_k. Moreover, the complete plasmonic response can be separated in a geometry-dependent part determined by χ_k, u_k, and v_k and a material-dependent part. In the more precise calculations based on the finite-difference time domain method [15] and on the boundary element method in the fully retarded cases [16] one cannot separate, at least directly, the geometry-dependent part from the material-dependent part. We note here that our BIE is valid in the quasi-static limit which holds as long as the NP size is much smaller than the wavelength of the incident light, typically NP size below $\lambda/10$ which is usually the case for chemically synthesized nanospheres [10].

3. Plasmonic properties of deformed metallic nanospheres

3.1 Numerical procedure
In order to calculate plasmonic properties of metallic nanoparticles we have used a numerical method that was presented in [14, 3]. The method is a spectral method with an exponential convergence [17]. Moreover, the method resembles the efficient fast multipole method of Rokhlin and Greengard [18,19]] since the use of a spherical harmonics related basis generates sparse and almost diagonal matrices of $\hat{M}$ and $\hat{S}$. Throughout this work we consider small variations from spherical shape of gold NPs immersed in water. The surface Σ is parameterized by $\{x = g(z)\cos\varphi, y = g(z)\sin\varphi, z\}$, where z and the angle φ are the variables that determine the surface and $g(z)$ is a smooth but otherwise arbitrary function, which has the following form:

$$g(z) = \frac{z_{max}}{1+az^2}\sqrt{1-(z/z_{max})^2} \; . \tag{8}$$

The parameters a and z_{max} determine the shape of an individual particle. We note here that the quasi-static theory is scale invariant, thus for our convenience we considered $z_{max}=2$. The spherical shape is given by $a = 0$. These shape changes however keep the aspect ratio unchanged. Without the factor z_{max} Eq. (4) can cover a much larger class of shapes including spheroids, nanodisks, or nanorods. The dielectric permittivity of gold is described by the Drude model with its parameters compiled from the literature. In the following sections we will analyze the LSPRs and the near-field enhancement of NPs that deviate smoothly from spherical shape. Specifically, we will study the shape determined by $a = 0.1$ that determines a volume variation of -13. % and a =-0.03 with a volume variation of 5%.
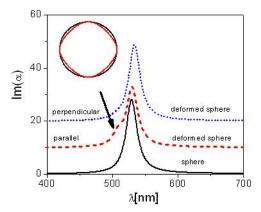

Fig. 1. The LSPR spectra of a simple and of a slightly deformed nanosphere (a=0.1). The solid line denotes the nanosphere and the dashed/dotted curve represents the deformed nanosphere in a field parallel/perpendicular to the Oz-axis. The inset shows the cross-sections of these two NPs. The spectra are shifted upward for a better visualization.

3.2 Deformed versus simple nanospheres. Plasmonic properties
In Fig. 1 there are presented the far-field spectral properties of a simple and of a deformed nanosphere with a volume variation of -13.% (a=0.1). The main LSPR is given by the dipole eigenmode in both cases. In the field parallel to the Oz-axis the deformed sphere shows, however, an additional LSPR, which is an octopole-like resonance. The new LSPR looks like a "hump" which is indicated by the arrow. On the other hand, in transverse field polarization (perpendicular to the Oz-axis) the spectra remain practically unchanged. The most representative eigenvalues and the weights w_k and n_k are given in Table 1. From Eq. (4) one can deduce that larger eigenvalues

χ_k means longer LSPR wavelengths, thus the dipole eigenvalue of the deformed nanosphere is slightly red-shifted with respect to the nanosphere.

Table 1. The most representative eigenmodes and their weights for a deformed nanosphere (a=0.1). The corresponding values for sphere are in parenthesis. The field is parallel to the symmetry axis.

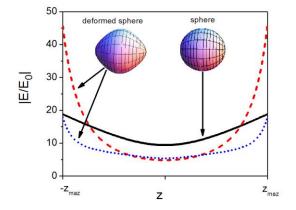| k	χ_k	w_k	n_k
1	0.5 (0.5)	0(0)	0(0)
2	0.1692(0.16667)	0.775(1)	2.7246(3.342)
3	0.143466 (0.1)	0(0)	1.5048 (0)
4	0.08147(0.07143)	0.18679(0)	0.6777(0)

Fig. 2. The near-field enhancement factors around a simple and around a slightly deformed nanosphere (a=0.1) at their resonance frequencies for the field parallel to the Oz-axis. The dipole mode enhancement of the perfect/deformed sphere is plotted with solid/dashed line. The near-field enhancement of the octopole mode of the deformed NP is depicted by a dashed line.

In contrast to the far-field, the shape variation has a bigger effect on the near-field enhancement. Fig. 2 shows the near-field enhancement around these two types of NPs at resonance frequency. The electric field polarization is parallel to the symmetry axis; therefore the near-field enhancement is also axially symmetric. The simple as well as the deformed nanosphere has the largest near-field enhancement created by the dipole eigenmode. One can see a much larger enhancement for the deformed NP with a maximum enhancement of 45. The nanosphere enhancement is just 19. In addition, the octopole enhancement of the deformed NP is comparable with the enhancement of the nanosphere.

In general, the field enhancement is determined by χ_k, the coupling factors n_k and the charge densities associated with each eigenmode. From Table 1 one can see a smaller value of n_k for the dipole mode therefore "spots" with larger field-enhancement implies "spots" with larger charge density. An additional contribution comes from the eigenmode $\chi_3 = 0.143466$ which is completely dark in the far-field ($w_3 = 0$) but has a consistent contribution in the near-field ($n_k = 1.5048$). The charge density of the dipole mode has its maximum along z-axis at the north/south pole. On the other hand, the deformed NP has a larger curvature in the regions with large field enhancement. This example suggests a modality to increase the near-field enhancement by modifying the curvature of the NP in the regions where the charge density of the eigenmode is maximal. Also it shows that BIE can easily identify concurring bright and dark eigenmodes for larger near-field enhancement in contrast to more rigorous and more complex method of [15] and [16].
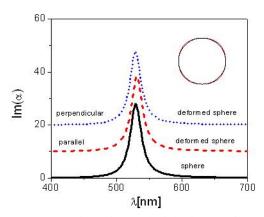
*Fig. 3. The LSPR spectra of a simple and of a slightly deformed nanosphere (a=-0.03).
The solid line denotes the nanosphere and the dashed/dotted curve represents the
deformed nanosphere in parallel/perpendicular polarization field. The inset shows the
cross-sections of these two NPs. The spectra are shifted upward for a better visualization.*

The second case is a slightly larger and deformed nanosphere with a=-0.03 and a volume variation of 5% bigger than of a corresponding simple nanosphere. In Fig. 3 there is shown the spectral dependence of the far-field, where no significant modification occurred by shape change. The corresponding eigenvalues and their weights are presented in Table 2. Like in the previous case the dipole LSPR of the deformed nanosphere is also red-shifted. In addition, there is at least one other eigenmode (an octopole-like) that has its weight different from zero, but the weight is not big enough to be noticeable in the spectrum [9]. Like in the previous case of deformed but smaller nanosphere the third eigenmode is dark in the far-field but has a non-vanishing contribution for the evanescent near-field.

*Table 2: The most representative eigenmodes and their weights for a deformed
nanosphere (a=-0.03). The corresponding values for sphere are in parenthesis. The field
is parallel to the symmetry axis.*

k	χ_k	w_k	n_k
1	0.5 (0.5)	0(0)	0(0)
2	0.1728 (0.16667)	0.98173(1)	3.363 (3.342)
3	0.08629(0.1)	0(0)	0.5267(0)
4	0.0645 (0.07143)	0.01809(0)	0.053(0)

Fig. 4 shows the near-field enhancement around these two types of NPs at the resonance frequencies. The electric field polarization is also parallel to the symmetry axis; therefore the near-field enhancement is symmetric about z-axis. The dipole eigenmode still induces the largest near-field enhancement in the deformed nanosphere but its value is smaller than the near-field created by a simple nanosphere. The near-field maximum is no longer along the z-axis as was the case of the smaller deformed nanosphere presented above.
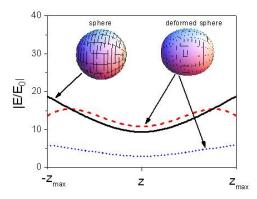
Fig 4. The near-field enhancement factors around a simple and around a slightly deformed nanosphere (a=-0.03) at their resonance frequencies for the field parallel to the Oz-axis. The dipole mode enhancement of the perfect/deformed sphere is plotted with solid/dashed line. The near-field enhancement of the octopole mode of the deformed NP is depicted by a dashed line.

Due to its bigger volume the deformed NP can surround the nanosphere, therefore its curvature is smaller than the curvature of a sphere along x-, y-, and z-axis. Thus the maximum of the dipole charge density is not along those axes, but along a direction where the curvature is smaller. Still, as suggested by the first example, the near-field enhancement of the deformed NP can be improved by further modifications of the curvature in the region where the near-field reaches its maximum.

4. Conclusions

The effect of shape variation on LSPR can be suitably studied with the BIE method. The BIE method allows continuous monitoring of the key aspects (eigenvalues, eigenfunctions, weights, etc.) of the LSPR with respect to the NP geometry. Slightly modifications of spherical shape show that the near-field enhancement is more affected by shape changes than the far-field spectrum. The near-field changes are determined by local curvature variations in the regions with large field enhancement. In contrast, the far-field is influenced by global geometry changes like the volume variations of more than 10%. The present calculations may explain why the nanospheres have shown significant results in SERS studies where a near-field enhancement of hundreds of times is needed [10]. Finally, this study provides some guidelines of designing plasmonic structures for sensing applications, where factors like the near-field enhancement and the extinction spectrum are needed to be easily determined and interpreted.

Acknowledgements

References

[1] D.R. Fredkin, I.D. Mayergoyz, Phys. Rev. Lett. **91**, 253902 (2003).
[2] T. Sandu, D. Vrinceanu, E. Gheorghiu, Plasmonics **6**, 407 (2011).
[3] T. Sandu, Plasmonics **8**, 391 (2013).
[4] K.M. Mayer, J.H. Hafner, Chem. Rev **111**, 3828 (2011).
[5] K.T. Yong, M.T. Swihart, H. Ding, P. Prasad, Plasmonics **4**, 79 (2009).
[6] J.Z. Zhang, J Phys Chem Lett **1**, 686 (2010).

[7] D. Grieser, H. Uecker, S. A. Biehs, O. Huth, F. Rüting, M. Holthaus, Phys Rev. B **80**, 245405 (2009).

[8] P. Ginzburg, N. Berkovitch, A. Nevet, I. Shor, M. Orenstein, Nano Lett. **11** , 2329 (2011).

[9] T. Sandu, J. Nanopart. Res. **14**, 905 (2012).

[10] P.K. Jain, M.A. El-Sayed, Chem. Phys. Lett. **487**, 153, (2010)

[11] I. Tsukerman, F. Čajko, J. Dai, NanoBioTechnology **3**, 148 (2007).

[12] T. W. Odom, C. L. Nehl, ACS Nano **2**, 612, (2008).

[13] M. A. Bratescu, S. -P. Cho, O. Takai, N. Saito, J. Phys. Chem. C **115**, 24569 (2011).

[14] T. Sandu, D. Vrinceanu, E. Gheorghiu, Phys. Rev. E **81**, 021913 (2010).

[15] C. Oubre, P Nordlander, J. Phys. Chem. B **108**, 17740 (2004).

[16] F. J. García de Abajo, A. Howie, Phys. Rev. B **65**, 115418 (2002).

[17] J. P. Boyd, Chebyshev and Fourier Spectral Methods. Dover, New York (2001).

[18] V. Rokhlin, J. Comput. Phys. **60**, 187 (1985).

[19] F. Greengard, V. Rokhlin, Acta Numerica **6**, 229 (1997).